



Simultaneous multi-wavelength observations of the repeating fast radio burst FRB 20190520B with Swift and FAST

ZHEN YAN ¹, WENFEI YU ¹, K.L. PAGE ², JIE LIN,^{3,4} DI LI,^{5,6,7} CHENHUI NIU,^{5,8} CASEY LAW,^{9,10}
BING ZHANG ^{11,12}, SHAMI CHATTERJEE,¹³ XIAN ZHANG ^{1,6} AND RESHMA ANNA-THOMAS ^{14,15}

¹Shanghai Astronomical Observatory, Chinese Academy of Sciences, 80 Nandan Road, Shanghai 200030, China

²School of Physics & Astronomy, University of Leicester, LE1 7RH, UK

³CAS Key laboratory for Research in Galaxies and Cosmology, Department of Astronomy, University of Science and Technology of China, Hefei 230026, China

⁴School of Astronomy and Space Sciences, University of Science and Technology of China, Hefei 230026, China

⁵National Astronomical Observatories, Chinese Academy of Sciences, Beijing 100012, China

⁶University of Chinese Academy of Sciences, 19A Yuquanlu, Beijing 100049, China

⁷Research Center for Intelligent Computing Platforms, Zhejiang Laboratory, Hangzhou 311100, China

⁸Institute of Astrophysics, Central China Normal University, Wuhan 430079, China

⁹Cahill Center for Astronomy and Astrophysics, MC 249-17 California Institute of Technology, Pasadena, CA 91125, USA

¹⁰Owens Valley Radio Observatory, California Institute of Technology, 100 Leighton Lane, Big Pine, CA, 93513, USA

¹¹The Nevada Center for Astrophysics, University of Nevada, Las Vegas, Las Vegas, NV 89154, USA

¹²Department of Physics and Astronomy, University of Nevada, Las Vegas, Las Vegas, NV 89154, USA

¹³Cornell Center for Astrophysics and Planetary Science, and Department of Astronomy, Cornell University, Ithaca, NY, USA.

¹⁴West Virginia University, Department of Physics and Astronomy, P.O. Box 6315, Morgantown, WV, USA

¹⁵Center for Gravitational Waves and Cosmology, West Virginia University, Chestnut Ridge Research Building, Morgantown, WV, USA

ABSTRACT

Fast radio bursts (FRBs) are bright, millisecond-duration radio bursts of cosmic origin. There have been several dozen FRBs found to repeat. Among them, those precisely localized provide the best opportunity to probe their multi-wavelength counterparts, local environment, and host galaxy that would reveal their origins. Here we report our X-ray, ultraviolet (UV) and optical observations with the *Swift* satellite that were performed simultaneously in the radio band with the Five-hundred-meter Aperture Spherical radio Telescope (FAST) observations of the repeating FRB 20190520B, aiming at detection of possible multi-wavelength bursts in association with radio bursts and multi-wavelength counterpart of the persistent radio source (PRS). While a total of 10 radio bursts were detected by FAST at the same time of *Swift* observations, we detected neither X-ray, UV or optical bursts in accompany of the radio bursts, nor persistent multi-wavelength counterpart of the PRS. We obtained the energy upper limits (3σ) on any multi-wavelength bursts as 5.03×10^{47} erg in the hard X-ray band (15–150 keV), 7.98×10^{45} erg in the soft X-ray band (0.3–10 keV), and 4.51×10^{44} erg in the U band (3465Å), respectively. The energy ratio between soft X-ray (0.3–10 keV) and radio emission of the bursts is constrained as $< 6 \times 10^7$, and the ratio between optical (U band) and radio as $< 1.19 \times 10^6$. The 3σ luminosity upper limits at the position of PRS are 1.04×10^{47} (15–150 keV), 8.81×10^{42} (0.3–10 keV), 9.26×10^{42} (UVW1), and 2.54×10^{42} erg s⁻¹ (U), respectively. We show that the PRS is much more radio loud than representative pulsar wind nebulae, supernova remnants, extended jet of Galactic X-ray binaries and ultraluminous X-ray sources, suggestive of boosted radio emission of the PRS.

1. INTRODUCTION

Fast radio bursts (FRBs) are radio bursts with a typical duration on the millisecond time scales that have

been observed with a dispersion measure (DM) larger than that of the Galactic values, indicating their cosmological origins. Their short duration has prevented them from being easily localized in the radio band; there have been more than 30 fine localized FRBs. The search for potential persistent and transient multi-wavelength counterparts through ground or space observations is

largely dependent on precise localizations on the arc-second scale or better.

The observed FRB population contains repeating FRBs and non-repeating FRBs, for which the relation between the two potential sub-categories and whether they are of distinct or same origins are not determined (see Zhang 2023, for a review). Among the entire FRB sample, the first known FRB with a persistent radio source (PRS) is identified by Chatterjee et al. (2017). The search for multi-wavelength counterparts, specifically high energy counterparts, has yielded non-detections (e.g. Scholz et al. 2017; Sun et al. 2019, 2021; Laha et al. 2022a,b). Although previous observations of other FRBs during their active phase, such as those of FRB 20121102A, have indicated that there are no persistent X-ray or optical point sources in association with the radio bursts in their corresponding host galaxies, it is still necessary to perform further observations of FRB targets like FRB 20190520B, since potential multi-wavelength counterparts, either short-lived or emerging persistently, could appear at a later time due to the potential trigger by its previous activity, as suggested by the observation of emerging radio flux following the outburst of the Galactic magnetar SGR 1935+2154 (Bochenek et al. 2020; Li et al. 2021a).

Five-hundred-meter Aperture Spherical Telescope (FAST; Nan et al. 2011) is equipped with 19-beams receiver to enlarge its field of view in L-band. FRB 20190520B was discovered from the archived data in Commensal Radio Astronomy FAST Survey (CRAFTS; Li et al. 2018; Li et al. 2019). It is an active repeating FRB source from which four bursts were detected in the drift scan survey. Three were detected in the same beam during the drift scan and the other one was followed up in another beam. By checking the beams pointing at the time of events, FAST observations have localized it to a position accuracy of a few arc-minutes. Through the VLA DDT/20A-557 program, we were able to localize the bursts to the sub-arcsecond accuracy with the discovery of a PRS in spatial association with the bursts and determine the redshift of the FRB 20190520B as 0.241 after identification of its host galaxy (Niu et al. 2022). With both refined burst and PRS positions, we then search for simultaneous or quasi-simultaneous multi-wavelength, persistent or short-lived counterparts.

FRB 20190520B has been persistently active ever since its discovery and remains the only such repeater without any extended (longer than a few days, e.g.) dormant epoch. FRB 20190520B is thus an ideal target to be followed up with multi-band observations. It also produced a lot of bursts with a high signal-to-noise ra-

tio ($S/N \sim$ a few tens) as seen with FAST in our campaign. Therefore multi-wavelength observations simultaneously or quasi-simultaneously with FAST observations would yield valuable upper limits or even potential detection of multi-wavelength bursts in temporal association with these radio bursts. Multi-wavelength bursts in association with those radio bursts would provide crucial information about the central engine of the FRB 20190520B (e.g. Nicastro et al. 2021; Zhang 2023), and thus reveal the nature of the repeating FRBs or the FRBs as a whole.

The *Swift* mission is flexibly scheduled and quickly responding for target-of-opportunity (ToO) observations of transient events in hard X-ray, soft X-ray, and ultraviolet (UV)/optical bands (Gehrels et al. 2004). It consists of three major instruments, namely, Burst Alert Telescope (BAT), X-Ray Telescope (XRT) and Ultraviolet/Optical Telescope (UVOT). BAT covers the hard X-ray band ($\sim 15\text{--}150$ keV) and is capable of searching for any bright hard X-ray bursts if the target is in its large field-of-view. XRT is a focusing X-ray telescope which covers the soft X-ray band (0.3–10 keV). The time resolution is 2.51 seconds and 1.8 milliseconds for the photon-counting (PC) and windowed-timing (WT) modes, respectively. It can detect potential soft X-ray bursts or a persistent X-ray counterpart. UVOT is equipped with six filters in the UV/optical band. It can collect event mode data with high time resolution (~ 12 milliseconds), which can detect potential UV/optical bursts and also any persistent counterpart.

Here we report our simultaneous *Swift* and FAST observations of the FRB 20190520B performed in May and August of 2020. In the *Swift* archive, there was a previous observation which covered the FRB 20190520B field-of-view (FoV) in 2016, which was triggered by a non-GRB event and pointed at about 5 arc-minutes away. This observation is also included in our analysis. We used the coordinates 16:02:04.266, -11:17:17.33 obtained from the VLA observation (Niu et al. 2022) in the following analysis for both burst (i.e., short-term, time-domain counterpart) and PRS searching. For the latter, we stacked multiple XRT and UVOT observations to generate deep images in the X-ray and optical band to achieve more stringent constraints on the persistent flux of the PRS.

2. OBSERVATIONS

We requested two sets of simultaneous *Swift* and FAST Target-of-Opportunity (ToO) observations of FRB 20190520B in May and August of 2020. The first *Swift*/FAST campaign in May 2020 was aimed at detecting potential X-ray bursts in both soft X-ray band

(XRT) and hard X-ray band (BAT) in association with the radio bursts that would be detected with a single FAST observation. The secondary goal of this campaign was to perform an initial investigation of the field in the UV wavelengths with *Swift*/UVOT and search for potential bursts as well. The second *Swift*/FAST campaign in August 2020 was primarily aimed at optical photometric observations performed simultaneously with FAST observations when our target was confirmed active and a sub-arcsecond localization was made by the VLA. All of the FAST observations were performed in tracking mode, with the May 2020 campaign pointed at the position then determined with previous FAST drift scan and tracking observations, and the August 2020 campaign pointed at the preliminary VLA localization of the radio bursts and the PRS achieved at the time of the observations.

2.1. FAST observations

The FAST observations coeval with the *Swift* observations were obtained through Director’s Discretionary Time (DDT2020_3) and the FAST key science project. Based on the initial coarse localization of FRB 20190520B based on the analysis of partially over-lapping drift scans as part of the CRAFTS design (Li et al. 2018), FAST observations of FRB 20190520B started on April 25, 2020, during which multiple bursts were detected successfully. On May 22, in the FAST observation that was jointly performed with *Swift*, 13 bursts were observed, further indicating that this source had been active. In late July, since our VLA DDT program had successfully localized the bursts to arc-second position accuracy, we requested an additional simultaneous campaign on FRB 20190520B with *Swift* and FAST by making use of the precise localization. The campaign lasted from 2020 August 4 to August 16, during which a total of 7 *Swift* observations were carried out once every two days (Table 1). During this period of time, 6 FAST observations are performed. FAST could track FRB 20190520B for ~ 1.7 hours each day due to the constraint by the observation window. In total, 40 radio bursts were detected at L band by FAST during this campaign (Niu et al. 2022), and 10 of which are covered by the time windows of the Swift observations (Table 5).

2.2. Swift observations

We requested a single *Swift* ToO observation on 2020 May 22 and seven observations during the first half of 2020 August. The first *Swift* observation made use of the updated FAST localization of the bursts with both drift scan and tracking observations up to May 2020.

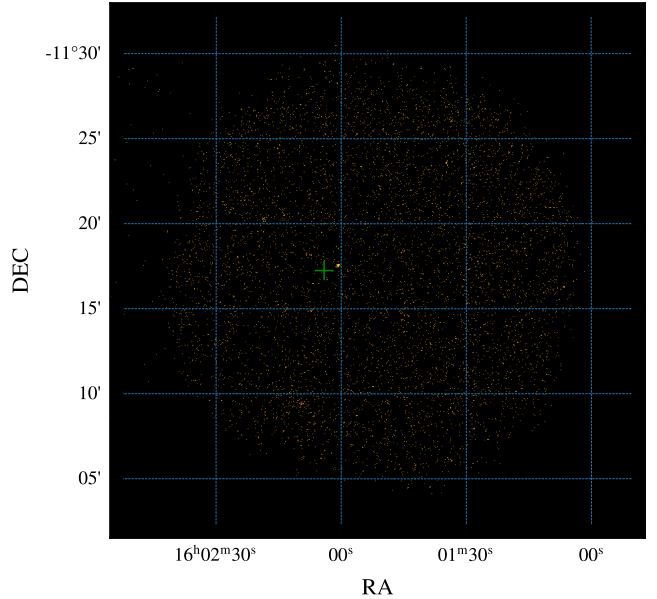


Figure 1. The stacked image of all the XRT observations. The green cross marks the FRB 20190520B position. The upper right bright point source is a bright star V* V1042 Sco.

The second campaign, which benefited from the results achieved from the first simultaneous *Swift* and FAST campaign, i.e., non-detection of any bursts with XRT and UVOT, as well as the refined localization obtained with the VLA localization of the bursts and identification of the PRS, was targeting at potential simultaneous fast optical bursts in association with the radio bursts down to the time scales as short as ~ 12 ms (event mode of UVOT). In addition to these eight observations, there was an archival *Swift* pointed observation which covered this source in its field-of-view in 2016. Specifically, all the *Swift*/XRT observations were performed in the PC mode. The information about all the *Swift* observations is listed in Table 1.

During the observation campaign in May, we proposed the BAT as the scientifically crucial instrument and set up the observation in event mode during the *Swift* observation. However, the BAT event data were not stored successfully. We then used the survey data to search for the persistent or long-lived hard X-ray counterpart. We also retrieved the *Swift*/BAT event data with exposure longer than 100 seconds and within 30° of the FRB 20190520B positions during the FAST observation period (MJD 58962–59112, the observation information is listed in Table 4).

3. DATA ANALYSIS AND RESULTS

3.1. upper limits on persistent emission

Table 1. The upper limits of the XRT and UVOT for each observation

obsID	start time (UTC)	exposure (s)	filter	AB Mag	Flux (μjy)	XRT rate (10^{-3} c/s)
00034397001	2016-02-27 22:58:04	744	U	> 21.73	< 7.50	< 12.39
00013503001	2020-05-22 17:09:35	1396	UVW1	> 22.24	< 4.54	< 6.31
00013503002	2020-08-04 11:29:35	1378	U	> 22.22	< 4.77	< 6.27
00013503003	2020-08-06 11:12:35	1669	U	> 22.33	< 4.33	< 5.22
00013503004	2020-08-08 10:57:34	1558	U	> 22.27	< 4.56	< 7.70
00013503005	2020-08-10 10:53:35	1411	U	> 22.15	< 5.10	< 6.37
00013503006	2020-08-12 10:39:35	1557	U	> 22.26	< 4.60	< 6.17
00013503007	2020-08-14 10:28:36	1398	U	> 22.19	< 4.89	< 5.80
00013503008	2020-08-16 11:42:35	1368	U	> 22.13	< 5.19	< 6.51

Note: All of them are 3σ upper limits.

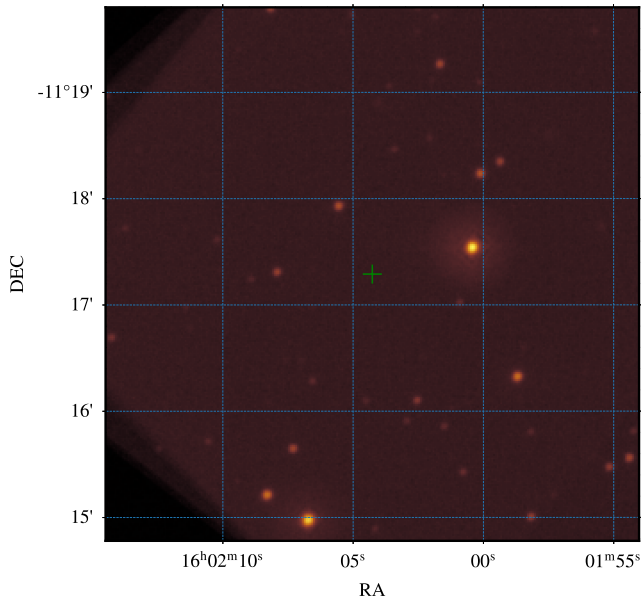


Figure 2. The stacked image in the U -band of UVOT. The green cross marks the FRB 20190520B position. The upper right brightest star corresponds to the nearby X-ray point source seen with XRT.

If we assume a power law X-ray spectrum with photon index of 2 and take the Galactic column density of hydrogen to be $2.6 \times 10^{21} \text{ cm}^{-2}$, 1 counts s^{-1} XRT rate corresponds to unabsorbed X-ray flux $5.77 \times 10^{-11} \text{ erg cm}^{-2} \text{ s}^{-1}$ in the 0.3–10 keV band, and 1 counts s^{-1} BAT rate corresponds to unabsorbed X-ray flux $8.33 \times 10^{-8} \text{ erg cm}^{-2} \text{ s}^{-1}$ in the 15–150 keV according to the conversion from WebPIMMS², which correspond to $9.94 \times 10^{45} \text{ erg s}^{-1}$ (0.3–10 keV) and $1.48 \times 10^{49} \text{ erg s}^{-1}$ (15–150 keV) for the distance of 1218 Mpc (Niu et al.

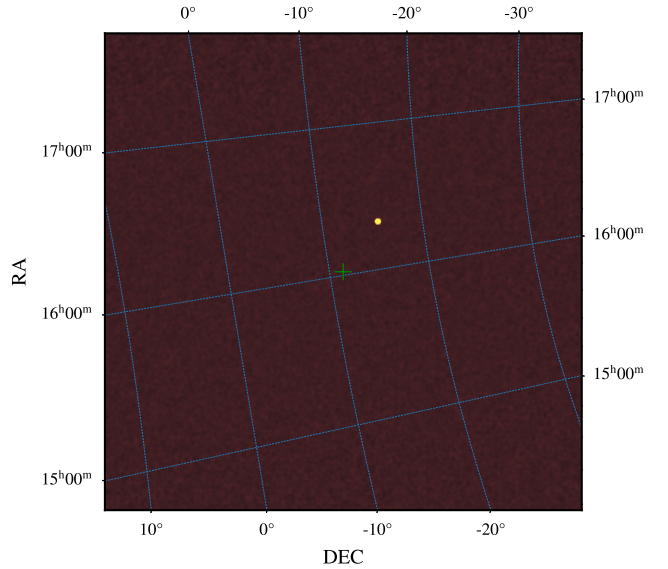


Figure 3. The *Swift*/BAT hard X-ray survey image obtained from obsID 00013503003. The bright persistent source is Sco X-1. The green cross marks the VLA position of FRB 20190520B.

2022). Then we can use this conversion to roughly estimate the X-ray flux in the following analysis.

For each Swift/XRT observation, we gave the 3σ upper limit by using the online Swift/XRT products generator³ (Evans et al. 2007), since there is no positive detection at the radio position of FRB 20190520B (Table 1). We also stacked all the XRT observations in 2020 and obtained the X-ray count rate upper limit as 8.6×10^{-4} c/s on the potential persistent source at the FRB 20190520B position. The limit on the 0.3–10 keV X-ray flux is $4.96 \times 10^{-14} \text{ erg cm}^{-2} \text{ s}^{-1}$ by using the above assumption, which corresponds to the X-ray lu-

¹ <https://www.swift.ac.uk/analysis/nhtot/index.php>

² <https://heasarc.gsfc.nasa.gov/Tools/w3pimms.html>

³ https://www.swift.ac.uk/user_objects/

minosity of 8.81×10^{42} erg s^{-1} . It is worth noting that there are only two photons detected within the PSF ($18''$) during the total ~ 12400 seconds exposure; there is an unrelated source detected near FRB 20190520B with XRT count rate $5.2 \pm 0.8 \times 10^{-3}$ c/s at a significance of about 6σ . The coordinate of the source is 16h02m00.6s,-11d17m32.9s obtained by using *sosta*, which is $56''$ far from FRB 20190520B (Figure 1). It is very bright in U-band (see Figure 2). We searched the SIMBAD Astronomical Database (Wenger et al. 2000) and found it is a bright star V* V1042 Sco.

For each *Swift*/UVOT observation, photometric analysis was performed by using the task *uvotsource* with a recommended aperture radius of $3''^4$. All the photometric results are listed in Table 1. None of the observations has yielded a positive detection of the persistent source at the VLA position of the FRB 20190520B. In order to obtain the limiting magnitude of our target, we stacked the images from the eight observations performed with the U filter (see Figure 2). We achieved a 3σ upper limit as 23.36 (AB magnitude) in the U-band on the persistent source at the FRB 20190520B position, corresponding to a luminosity of 2.54×10^{42} erg s^{-1} . There is only one observation performed with the UVW1 filter; the upper limit is 22.25 (AB magnitude), corresponding to 9.26×10^{42} erg s^{-1} .

We reduced the BAT event data following the standard analysis threads introduced by UK *Swift* Science Data Centre⁵. The survey data were processed with the *batsurvey* script. We then used *batcelldetect* to extract the signal-to-noise ratio (SNR) at the FRB 20190520B position in BAT sky images. The best SNR is 2.3σ , which is far below the recommended detection threshold of 5σ . The 3σ upper limit estimated from background is about 0.007 counts s^{-1} cm^{-2} (15–150 keV) with exposure time 1677 seconds, which corresponds to the X-ray flux of 5.83×10^{-10} erg s^{-1} cm^{-2} by assuming a power-law spectrum with index of 2, and the X-ray luminosity of 1.04×10^{47} erg s^{-1} .

We then plotted the broad band spectral energy distribution (SED, Figure 4) by adopting the persistent radio flux $202 \pm 8 \mu Jy$, and the extinction $E(B - V) = 0.26$ is used (Niu et al. 2022).

3.2. upper limits on the burst emission

We also estimate the upper limits on the simultaneous X-ray and optical fluxes of the radio burst detected by FAST (Niu et al. 2022). The dispersion delay corre-

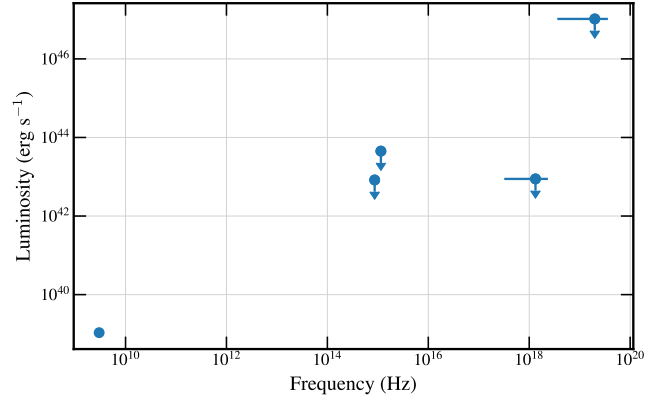


Figure 4. The broad band SED of the PRS of the FRB 20190520B. The radio luminosity is from Niu et al. (2022), the upper limits on other wavelengths are constrained in this work.

sponding to infinite frequency is calculated by using the DM in Table 5. Then a correction of time is made afterwards to search for the potential simultaneous bursts at X-ray and optical bands.

In order to search for simultaneous hard X-ray bursts, we extracted the light curves (15–150 keV) from *Swift*/BAT event data with time resolution of 10 ms by using the tool *batbinevt*. We then searched for simultaneous X-ray bursts in the 15–150 keV band on 10 ms time scale. This time scale was chosen because it is comparable to typical duration of the FRBs seen with FAST while also helps compromise photon statistics for the burst search. However, none of the radio bursts has been covered by the *Swift*/BAT event data within 1000 seconds.

We then used the standard deviation of the count rate on timescale of 10 ms to estimate the 3σ upper limit on potential X-ray bursts as 3.40 counts s^{-1} cm^{-2} , which corresponds to the X-ray flux of 2.83×10^{-7} erg s^{-1} cm^{-2} by assuming the power law index of 2, and the luminosity of 5.03×10^{49} erg s^{-1} and the energy of 5.03×10^{47} erg.

In order to estimate the soft X-ray upper limit on each radio burst detected by FAST, we used the online tool (Evans et al. 2007) to generate the light curve of each observation with a time resolution of 2.51 seconds. There are a total of 10 radio bursts which were simultaneously covered by the *Swift*/XRT observations; the upper limits of XRT count rate are listed in the Table 2. The corresponding upper limits on X-ray luminosity and energy are roughly estimated as 3.28 – 3.72×10^{46} erg s^{-1} , and 8.22 – 9.34×10^{46} erg (Table 2). We also searched for potential flares during the 100s interval around each radio burst. There is no positive detection, and the upper limit is roughly in the above range.

⁴ https://swift.gsfc.nasa.gov/analysis/threads/uvot_thread_aperture.html

⁵ <https://www.swift.ac.uk/analysis/bat/index.php>

Table 2. Burst upper limit from XRT on time scale of 2.51s.

burst time ^a (MJD)	XRT time (MJD)	Count Rate ^b (c/s)	Luminosity (10^{46} erg s ⁻¹)	Energy (10^{46} erg)	E_X/E_R ^c $\times 10^8$
58991.728910176	58991.728923501	<3.58	<3.66	<9.19	<5.47
59067.484320871	59067.484320859	<3.45	<3.53	<8.87	<5.58
59067.484321450	59067.484320859	<3.45	<3.53	<8.87	<4.98
59071.470478456	59071.470485296	<3.63	<3.72	<9.34	<9.73
59071.470478688	59071.470485296	<3.63	<3.72	<9.34	<11.54
59075.452687489	59075.452698807	<3.20	<3.28	<8.22	<2.16
59075.453197005	59075.453192673	<3.20	<3.28	<8.23	<3.23
59077.496337171	59077.496344162	<3.53	<3.62	<9.08	<5.41
59077.496488380	59077.496489417	<3.54	<3.63	<9.10	<8.35
59077.497491638	59077.497477148	<3.54	<3.62	<9.10	<7.98

^a The burst time is at Coordinated Universal Time (UTC), which is referenced to infinite frequency.

^b This is 3σ upper limit.

^c The ratio between X-ray and radio energy.

Table 3. Burst upper limit in the U -band on time scale of 12 ms

burst time ^a (MJD)	U time (MJD)	AB Mag ^b	Luminosity (10^{46} erg s ⁻¹)	Energy (10^{44} erg)	E_U/E_R ^c $\times 10^6$
59067.484320871	59067.484320927	<12.93	<3.76	<4.51	<2.83
59067.484321450	59067.484321482	<12.93	<3.76	<4.51	<2.53
59071.470478456	59071.470478477	<12.93	<3.76	<4.51	<4.70
59071.470478688	59071.470478755	<12.93	<3.76	<4.51	<5.56
59075.452687489	59075.452687499	<12.93	<3.76	<4.51	<1.19
59075.453197005	59075.453196944	<12.93	<3.76	<4.51	<1.77
59077.496337171	59077.496337235	<12.93	<3.76	<4.51	<2.68
59077.496488380	59077.496488346	<12.93	<3.76	<4.51	<4.14
59077.497491638	59077.497491680	<12.93	<3.76	<4.51	<3.95

^a The burst time is at Coordinated Universal Time (UTC), which is referenced to infinite frequency.

^b This is 3σ upper/lower limit. The time resolution of the U -band is 12 ms.

^c The ratio between U -band and radio energy.

We then extracted available *Swift*/XRT images coincident with the radio burst with a time resolution of 2.51 seconds by using `xselect`. The corresponding exposure maps are also produced. Then we stacked all the 10 X-ray sky images and exposure maps, and obtained a 3σ upper limit as 0.32 counts s⁻¹ by using the tool `sosta`, which corresponds to an luminosity upper limit of 3.18×10^{45} erg s⁻¹, and an energy upper limit of 7.98×10^{45} erg.

We also notice that the DM is very large ~ 1200 pc cm⁻³ for FRB 20190520B. According to the correlation between the DM and X-ray column density in He et al. (2013), the corresponding column density of FRB 20190520B is about 3.6×10^{22} cm⁻². The unabsorbed X-ray flux as seen with the XRT in the 0.3–10 keV band is about four times larger than the previous es-

timination based on Galactic column density in the source direction alone. The unabsorbed X-ray flux as seen with BAT in the 15–150 keV range remains unchanged. However, the origin of DM is still uncertain for the bursts (Niu et al. 2022) and the local contribution is still significant (Lee et al. 2023). For order of magnitude estimation, we then still use the X-ray flux upper limits based on Galactic column density in the following.

One of the aims of the 2020 August campaign is fast photometry in the optical band. There were seven *Swift*/UVOT observations with U filter (3465Å) performed in event mode. We first made use of `uvotscreen` to obtain the corresponding cleaned event data. The astrometry of the event data is then refined by using the method in Oates et al. (2009). We extracted U -band images every 100 s. The position of each event was cor-

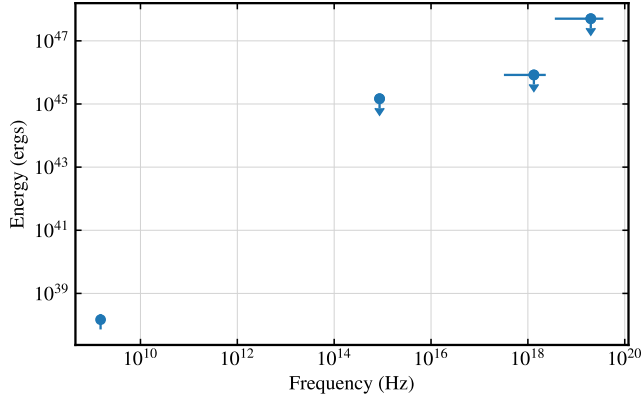


Figure 5. The broad band SED of burst emission of FRB 20190520B. The radio energy is averaged from the burst list in Niu et al. (2022), the upper limits on other wavelengths are constrained in this work.

rected by the differences obtained from cross-correlating the image with the USNO-B1 catalogue. We then used the task `uvotevtlc` to generate the corresponding light curve with time bin of 12 milliseconds from each event file by applying a circular source region with a radius of $3''$. As a result, the upper limits on the source flux in the time bins of 12 milliseconds, which was simultaneous with any radio burst detected by FAST observations, were thus obtained. The upper limits on the luminosity and burst energy on the time scale of 12 ms of 9 available bursts are $3.76 \times 10^{46} \text{ erg s}^{-1}$ and $4.51 \times 10^{44} \text{ erg}$ (Table 3). We also searched the 100s interval around the radio burst, there is no positive detection, and the upper limit is also the same as in Table 3.

We then use the burst energy upper limit extracted from the stacked XRT images, BAT event data and U band event data to plot the broad band SED of the burst emission in Figure 5. The average burst energy in 1.5 GHz and $E(B-V)=0.258$ is adopted (Niu et al. 2022).

Making use the average radio burst energy in Niu et al. (2022) and the X-ray burst energy upper limit from stacked XRT images, we derived the upper limit of the X-ray-to-radio energy ratio $E_X/E_R < 6 \times 10^7$. We also used the data of Table 4 of Laha et al. (2022b) to replot the relation between E_R and E_X (Figure 6).

4. SUMMARY AND DISCUSSION

Repeating FRBs provide great opportunity for burst localization and the search for multi-wavelength counterparts. In the past few years, however, significant challenges in the quest to detect multi-wavelength counterparts of FRBs from space or on the ground remain (Sun et al. 2019). We have performed simultaneous *Swift* pointed observations with FAST tracking observations in May and August 2020 of the actively repeating fast

radio burst FRB 20190520B, which is the second known FRB associated with a compact PRS. The properties of the radio bursts and the PRS have been reported in the discovery paper by Niu et al. (2022) as well as in Anna-Thomas et al. (2023) and Zhang et al. (2023). Here, we report our *Swift* campaign on both the bursts and the PRS. We manage to put constraints on potential multi-wavelength counterparts of the fast radio bursts and the PRS by making use of both short and long exposures of the XRT and UVOT on board *Swift*, following the precise localization of the bursting source by the VLA in 2020.

4.1. Burst counterparts

There are more than 60 radio bursts detected by FAST during this campaign, 10 of which were covered simultaneously by *Swift* observations (Table 5). We have obtained the short timescale flux upper limits in X-ray (2.51 seconds) and optical (U-band, 12 milliseconds) bands for the bursts (subsection 3.2). No soft X-ray or optical burst events were detected. Current measurements are limited by corresponding instrumental sensitivity on short timescales.

Chen et al. (2020) has estimated the ratio η , which represents the energy of FRB counterparts at various wavelengths compared to the radio wavelength, based on the non-detection achieved from different surveys and instruments. The ratio at different wavelengths is very helpful to constrain the emission models. We give the lower limit of the ratio $\eta = E_X/E_R \lesssim 6 \times 10^7$ and $\eta = E_U/E_R \lesssim 10^6$ (Figure 6, Table 3).

The discovery of Galactic FRB 20200428 from SGR 1935+2151 (Bochenek et al. 2020) suggests potential magnetar origin for FRBs, while the energy budget remains a major concern for magnetar models. FRB 20200428 is weaker than most of the FRBs by orders of magnitude. On the other hand, thousands of bursts from FRB 20121102A had been observed within a time span of 60 days, adding up to a substantial fraction of total available magnetic energy from a magnetar (Li et al. 2021b). The burst activities of FRB 20190520B would impose stronger challenges due to its long-lasting burst activity. There are in general two types of emission models within the magnetar nature of FRBs, those invoking emission inside the magnetosphere of the magnetar (e.g. Kumar et al. 2017; Yang & Zhang 2018; Lu et al. 2020) and those invoking relativistic shocks outside the magnetosphere (e.g. Lyubarsky 2014; Metzger et al. 2019; Beloborodov 2020). The latter type of model predicts a relatively large E_X/E_R (Sironi et al. 2021). The former type of model, on the other hand, can allow a smaller E_X/E_R (Zhang 2020). Our constraint on

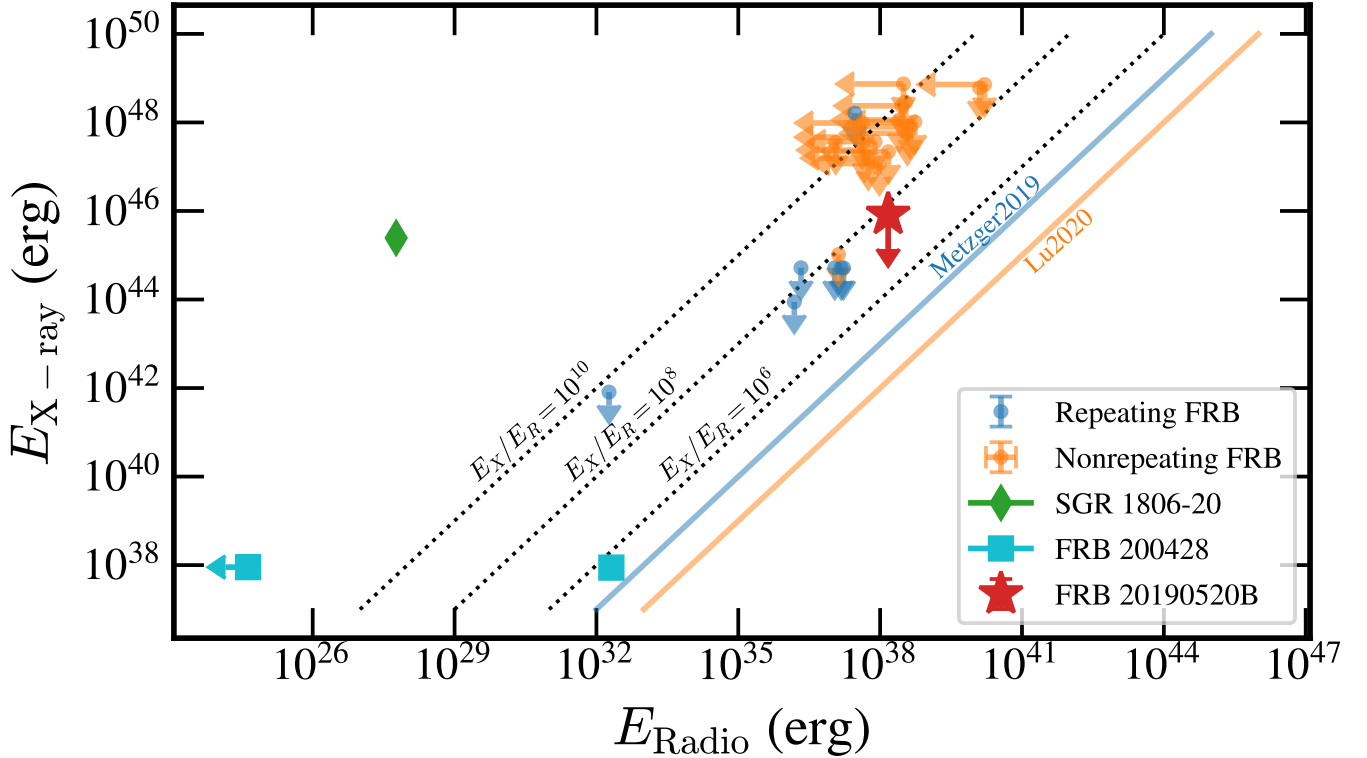


Figure 6. The relation between X-ray and radio energy of bursts in the FRBs. The data except that of FRB 20190520B are taken from Laha et al. (2022b). The blue and orange lines are the model prediction from Metzger et al. (2019) and Lu et al. (2020)

FRB 20190520B is much larger than the prediction of the two kind of models (Figure 6, see also Chen et al. 2020). More sensitive X-ray/optical telescopes are required for current FRB samples, or only the very nearby extragalactic optical/X-ray bursts are observable if current model predictions are correct.

4.2. PRS counterpart

The nature of the PRS in association with the FRB 20190520B (Niu et al. 2022) has peculiar variability properties, which are suggestive of an accreting compact object scenario (Zhang et al. 2023). To put a constraint on the multi-wavelength counterpart is crucial to reveal and determine the nature of the PRS. We have stacked all the XRT observations to obtain an upper limits on the persistent flux of 8.81×10^{42} erg s $^{-1}$. The upper limit on a potential persistent counterpart is obtained as 2.54×10^{42} erg s $^{-1}$ at U band and 9.26×10^{42} erg s $^{-1}$ at UVW1 band.

As the two most active FRBs to date and the best known FRBs with an PRS association, FRB 20190520B and FRB 20121102A share striking similarities in their burst environment. Their hosts are both dwarf galaxies with high star forming rate (Chatterjee et al. 2017; Niu et al. 2022). They are both

associated with a compact PRS. If the central engine is a magnetar, the PRS would correspond to a pulsar wind nebula (PWN) or a supernova remnant (SNR). However, the radio flux and spectra of the PRSs show evidence of variation on timescales as short as days, which indicates that the nature of a significant fraction of the instant PRS radio emission may come from accretion onto a compact object (Zhang et al. 2023; Rhodes et al. 2023). Their extremely large and variable rotation measures indicate that they are within dynamic, highly magnetized environments (Michilli et al. 2018; Anna-Thomas et al. 2023). On the other hand, a binary behind FRB sources has been suggested. The periodic activity of FRB 20121102A (Rajwade et al. 2020) and the sign reversal of the rotation measure of FRB 20190520B (Anna-Thomas et al. 2023) have invoked models of a binary system. Sridhar & Metzger (2022) have proposed the scenario in which a nebula surrounding the hyper-accretion X-ray binary (like ultraluminous X-ray source; ULX) may correspond to the PRS of the FRB. In this scenario, there should be a persistent X-ray counterpart to account for the ULX origin. Many of the radio properties of the PRS of the FRB 20190520B are consistent with the hyper-

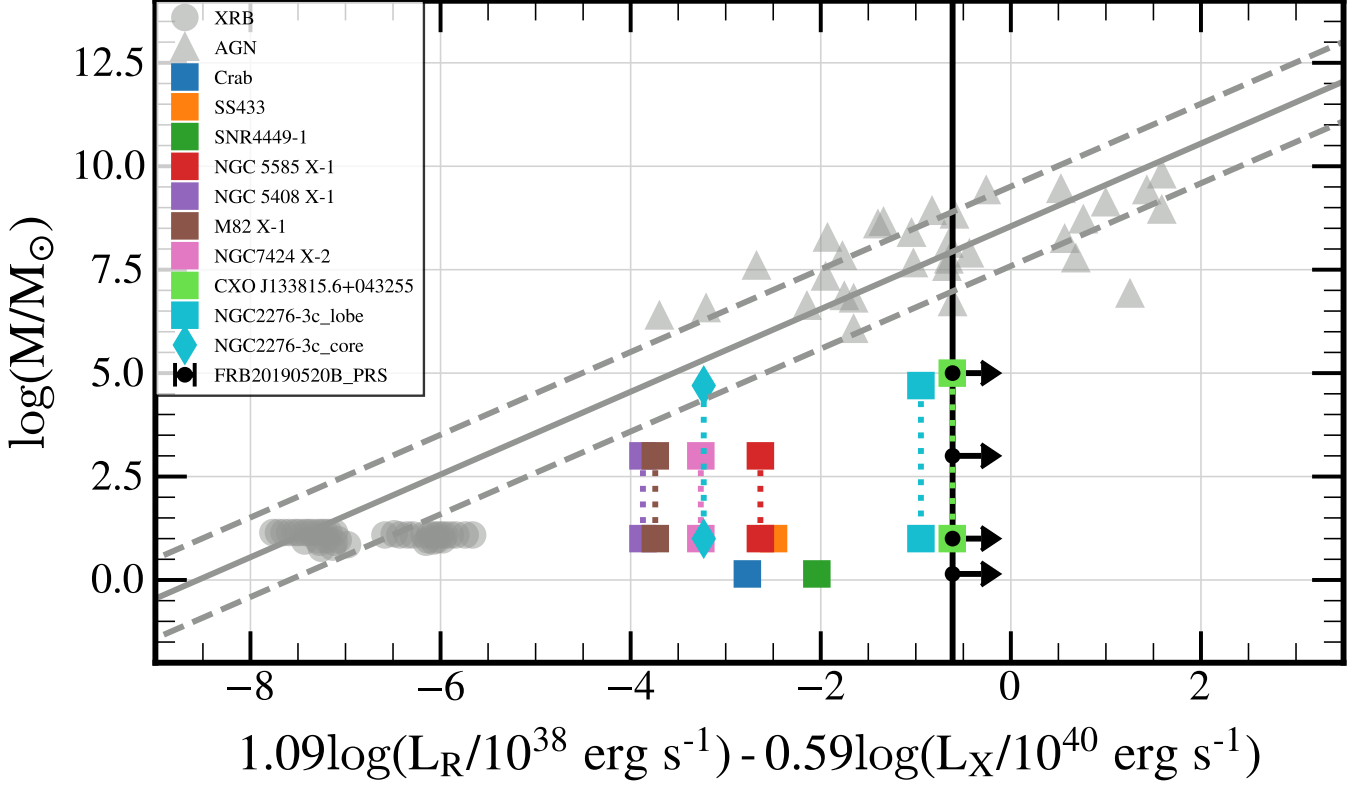


Figure 7. The gray data, solid and dashed lines represent the data of XRBs, AGNs and best-fitting results of the fundamental plane of accretion and jet activity of different scales of BHs. Different kinds of systems are also plotted in this diagram, including PWN, SNR, XRB nebula and ULXs. Solid black line represent the lower limit of FRB 20190520B, and the black dots with arrows are assumed BH masses of 10^5 , 10^3 , 10 and $1.4 M_{\odot}$.

accretion binary scenario when the apparent radio variability (Zhang et al. 2023) is attributed to scintillation (Bhandari et al. 2023).

If the source behind the PRS is an accreting compact object in a binary, not limited to hyper-accretion systems, we can compare the limits we obtained in the radio and X-ray band with accreting black holes and neutron stars. There is an established, empirical fundamental plane that describes black hole (BH) accretion and jet activities, i.e., a universal correlation between X-ray luminosity, radio luminosity and BH mass among accreting BHs of a wide range of mass scales, including X-ray binaries (XRBs) and active galactic nuclei (AGNs). We replotted the fundamental plane by using the data and best-fitting result of Gültekin et al. (2019). To show some other representative systems, we also added the data of Crab nebula (Lyutikov et al. 2019), an extragalactic SNR (Mezcua et al. 2013), a nebula of Galactic XRB SS 433 (Wolter et al. 2015) and some extragalactic ULXs (Laor & Behar 2008; Mezcua et al. 2015, 2018; Soria et al. 2021). Since ULXs are thought to be intermediate-mass black hole (IMBH) candidates or super-Eddington stellar mass accretion systems (some

are X-ray pulsars), we plotted both $10 M_{\odot}$ BH mass and the mass estimations in the literature or $1000 M_{\odot}$ for the ULX sample. The nature of the radio bubbles surrounding ULXs are still under debate. Some of them are considered to be jet emission, which are more radio loud than that of nebula. Especially when high resolution VLBI observations are performed, the jet structures can be resolved. For example, the radio core and large-scale radio lobe has been detected along the same direction in NGC 2276-3c (Mezcua et al. 2015). The radio core emission follows that established by the fundamental plane if the BH mass is about $5 \times 10^4 M_{\odot}$. Two radio lobes have also been observed in the ULX CXO J133815.6+043255 in NGC 5252. The total radio emission of both sources is thought to come from an extended jet rather than a compact jet.

Since the position of the PRS of FRB 20190520B is off-nuclear (Niu et al. 2022), its radio emission can not be due to the activity of the central super-massive BH suspected in the dwarf galaxy. The BH mass, if the PRS is powered by such a BH accreting system, should be less than $10^6 M_{\odot}$ (see also Zhang et al. 2023). So we used different mass quantities 1.4 , 10 , 10^3 and $10^5 M_{\odot}$ as the

possible mass of the compact object in the PRS when plotting the PRS of FRB 20190520B in Figure 7. In the diagram of Figure 7, the PRS of FRB 20190520B is much more radio loud than the brightest SNR, Crab nebula, SS433 and several ULXs. It is worth noting that the two ULXs with extended radio jets detected (namely CXO J133815.6+043255 and NGC 2276-3c) are quite close to the lower limit of the PRS of FRB 20190520B as seen in our plot. The radio spectral index of the PRS of FRB 20190520B is -0.4 ± 0.06 (Zhang et al. 2023), which is similar to the extended jet of the two ULXs (-0.5 ± 0.2 for NGC 2276-3c and -0.66 ± 0.02 for CXO J133815.6+043255; Mezcua et al. 2015; Smith et al. 2023). However, the radio luminosity of the PRS ($\sim 10^{39}$ erg s $^{-1}$) is still two orders of magnitude larger than that of the radio jets of the two ULXs ($\sim 10^{37}$ erg s $^{-1}$), which means the PRS of FRB 20190520B should either have a much more luminous radio jet or the observed radio jet emission is beamed and significantly boosted if our source is like a ULX of such kind, as also discussed for accreting systems with uncertain range of masses of the compact objects (Zhang et al. 2023). It is worth noting that the rare association of PRSs with FRBs in the entire FRB population (e.g., only two or three cases out of a thousand or more FRBs) while many FRBs closer than FRB 20190520B and FRB 20121102A have not been found associated with a PRS can be explained straight-forwardly if the radio emission of FRB 20190520B is beamed in a small solid angle (on the order of $1/1000$ of 4π) and boosted by relativistic effects.

In summary, we performed simultaneous Swift and FAST observations of FRB 20190520B. During our campaigns, 10 FRBs detected by FAST were covered by Swift XRT and UVOT observations. We have searched for potential burst emission on short timescale of 10 ms

(BAT 15–150 keV), 2.5 s (XRT: 0.3–10 keV) and 12 ms (UVOT: U band at 3465Å), and obtained the 3σ energy upper limits as 5.03×10^{47} erg, 7.98×10^{45} erg and 4.51×10^{44} erg, respectively. Using Swift/BAT’s survey observations and stacked XRT/UVOT observations, we also have obtained the 3σ luminosity upper limits of the multi-wavelength PRS counterpart as 1.04×10^{47} (15–150 keV), 8.81×10^{42} (0.3–10 keV), 9.26×10^{42} (U) and 2.54×10^{42} erg s $^{-1}$ (U), respectively. Based on these measured limits, we show the PRS of FRB 20190520B is much more radio loud than proposed FRB origins such as pulsar wind nebulae, supernova remnants and ultra-luminous X-ray sources (see Figure 7), suggestive of boosted radio emission from the PRS if the source is actually one of those objects as being proposed for the FRB.

WY would like to thank the Swift PI, Brad Cenko (and his designate) for approving and scheduling our Swift observations. We appreciate the Swift team for helping with quick data access. We would like to thank the FAST TAC to approve our DDT observations and the FRB Key Science Project for the arrangement of half of the FAST observations that are reported in this paper. WY, ZY and DL would like to acknowledge support by the National Natural Science Foundation of China (grant number 11333005, U1838203, U1938114, 11988101, 12373049 and 12373050). ZY was also supported in part by the Youth Innovation Promotion Association of Chinese Academy of Sciences. DL is a New Cornerstone Investigator. KLP acknowledges funding from the UK Space Agency.

Facilities: Swift, FAST

Software: astropy (Astropy Collaboration et al. 2018), matplotlib, proplot(Davis 2021),HEASoft

REFERENCES

- Anna-Thomas, R., Connor, L., Dai, S., et al. 2023, *Science*, 380, 599, doi: [10.1126/science.abo6526](https://doi.org/10.1126/science.abo6526)
- Astropy Collaboration, Price-Whelan, A. M., Sipőcz, B. M., et al. 2018, *AJ*, 156, 123, doi: [10.3847/1538-3881/aabc4f](https://doi.org/10.3847/1538-3881/aabc4f)
- Beloborodov, A. M. 2020, *ApJ*, 896, 142, doi: [10.3847/1538-4357/ab83eb](https://doi.org/10.3847/1538-4357/ab83eb)
- Bhandari, S., Marcote, B., Sridhar, N., et al. 2023, *ApJL*, 958, L19, doi: [10.3847/2041-8213/ad083f](https://doi.org/10.3847/2041-8213/ad083f)
- Bochenek, C. D., Ravi, V., Belov, K. V., et al. 2020, *Nature*, 587, 59, doi: [10.1038/s41586-020-2872-x](https://doi.org/10.1038/s41586-020-2872-x)
- Chatterjee, S., Law, C. J., Wharton, R. S., et al. 2017, *Nature*, 541, 58, doi: [10.1038/nature20797](https://doi.org/10.1038/nature20797)
- Chen, G., Ravi, V., & Lu, W. 2020, *The Astrophysical Journal*, 897, 146, doi: [10.3847/1538-4357/ab982b](https://doi.org/10.3847/1538-4357/ab982b)
- Davis, L. L. B. 2021, ProPlot, v0.9.5, Zenodo, doi: [10.5281/zenodo.5602155](https://doi.org/10.5281/zenodo.5602155)
- Evans, P. A., Beardmore, A. P., Page, K. L., et al. 2007, *A&A*, 469, 379, doi: [10.1051/0004-6361:20077530](https://doi.org/10.1051/0004-6361:20077530)
- Gehrels, N., Chincarini, G., Giommi, P., et al. 2004, *ApJ*, 611, 1005, doi: [10.1086/422091](https://doi.org/10.1086/422091)

- Gültekin, K., King, A. L., Cackett, E. M., et al. 2019, *ApJ*, 871, 80, doi: [10.3847/1538-4357/aaf6b9](https://doi.org/10.3847/1538-4357/aaf6b9)
- He, C., Ng, C. Y., & Kaspi, V. M. 2013, *ApJ*, 768, 64, doi: [10.1088/0004-637X/768/1/64](https://doi.org/10.1088/0004-637X/768/1/64)
- Kumar, P., Lu, W., & Bhattacharya, M. 2017, *MNRAS*, 468, 2726, doi: [10.1093/mnras/stx665](https://doi.org/10.1093/mnras/stx665)
- Laha, S., Wadiasingh, Z., Parsotan, T., et al. 2022a, *The Astrophysical Journal*, 929, 173, doi: [10.3847/1538-4357/ac5f3c](https://doi.org/10.3847/1538-4357/ac5f3c)
- Laha, S., Younes, G., Wadiasingh, Z., et al. 2022b, *The Astrophysical Journal*, 930, 172, doi: [10.3847/1538-4357/ac63a8](https://doi.org/10.3847/1538-4357/ac63a8)
- Laor, A., & Behar, E. 2008, *MNRAS*, 390, 847, doi: [10.1111/j.1365-2966.2008.13806.x](https://doi.org/10.1111/j.1365-2966.2008.13806.x)
- Lee, K.-G., Khrykin, I. S., Simha, S., et al. 2023, *ApJL*, 954, L7, doi: [10.3847/2041-8213/acefb5](https://doi.org/10.3847/2041-8213/acefb5)
- Li, C. K., Lin, L., Xiong, S. L., et al. 2021a, *Nature Astronomy*, 5, 378, doi: [10.1038/s41550-021-01302-6](https://doi.org/10.1038/s41550-021-01302-6)
- Li, D., Dickey, J. M., & Liu, S. 2019, *Research in Astronomy and Astrophysics*, 19, 016, doi: [10.1088/1674-4527/19/2/16](https://doi.org/10.1088/1674-4527/19/2/16)
- Li, D., Wang, P., Qian, L., et al. 2018, *IEEE Microwave Magazine*, 19, 112, doi: [10.1109/MMM.2018.2802178](https://doi.org/10.1109/MMM.2018.2802178)
- Li, D., Wang, P., Zhu, W. W., et al. 2021b, *Nature*, 598, 267, doi: [10.1038/s41586-021-03878-5](https://doi.org/10.1038/s41586-021-03878-5)
- Lu, W., Kumar, P., & Zhang, B. 2020, *MNRAS*, 498, 1397, doi: [10.1093/mnras/staa2450](https://doi.org/10.1093/mnras/staa2450)
- Lyubarsky, Y. 2014, *MNRAS*, 442, L9, doi: [10.1093/mnrasl/slu046](https://doi.org/10.1093/mnrasl/slu046)
- Lyutikov, M., Temim, T., Komissarov, S., et al. 2019, *MNRAS*, 489, 2403, doi: [10.1093/mnras/stz2023](https://doi.org/10.1093/mnras/stz2023)
- Metzger, B. D., Margalit, B., & Sironi, L. 2019, *MNRAS*, 485, 4091, doi: [10.1093/mnras/stz700](https://doi.org/10.1093/mnras/stz700)
- Mezcua, M., Kim, M., Ho, L. C., & Lonsdale, C. J. 2018, *MNRAS*, 480, L74, doi: [10.1093/mnrasl/sly130](https://doi.org/10.1093/mnrasl/sly130)
- Mezcua, M., Lobanov, A. P., & Martí-Vidal, I. 2013, *MNRAS*, 436, 2454, doi: [10.1093/mnras/stt1738](https://doi.org/10.1093/mnras/stt1738)
- Mezcua, M., Roberts, T. P., Lobanov, A. P., & Sutton, A. D. 2015, *MNRAS*, 448, 1893, doi: [10.1093/mnras/stv143](https://doi.org/10.1093/mnras/stv143)
- Michilli, D., Seymour, A., Hessels, J. W. T., et al. 2018, *Nature*, 553, 182, doi: [10.1038/nature25149](https://doi.org/10.1038/nature25149)
- Nan, R., Li, D., Jin, C., et al. 2011, *International Journal of Modern Physics D*, 20, 989, doi: [10.1142/S0218271811019335](https://doi.org/10.1142/S0218271811019335)
- Nicastro, L., Guidorzi, C., Palazzi, E., et al. 2021, *Universe*, 7, 76, doi: [10.3390/universe7030076](https://doi.org/10.3390/universe7030076)
- Niu, C. H., Aggarwal, K., Li, D., et al. 2022, *Nature*, 606, 873, doi: [10.1038/s41586-022-04755-5](https://doi.org/10.1038/s41586-022-04755-5)
- Oates, S. R., Page, M. J., Schady, P., et al. 2009, *MNRAS*, 395, 490, doi: [10.1111/j.1365-2966.2009.14544.x](https://doi.org/10.1111/j.1365-2966.2009.14544.x)
- Rajwade, K. M., Mickaliger, M. B., Stappers, B. W., et al. 2020, *MNRAS*, 495, 3551, doi: [10.1093/mnras/staa1237](https://doi.org/10.1093/mnras/staa1237)
- Rhodes, L., Caleb, M., Stappers, B. W., et al. 2023, *MNRAS*, 525, 3626, doi: [10.1093/mnras/stad2438](https://doi.org/10.1093/mnras/stad2438)
- Scholz, P., Bogdanov, S., Hessels, J. W. T., et al. 2017, *ApJ*, 846, 80, doi: [10.3847/1538-4357/aa8456](https://doi.org/10.3847/1538-4357/aa8456)
- Sironi, L., Plotnikov, I., Nättilä, J., & Beloborodov, A. M. 2021, *PhRvL*, 127, 035101, doi: [10.1103/PhysRevLett.127.035101](https://doi.org/10.1103/PhysRevLett.127.035101)
- Smith, K. L., Magno, M., & Tripathi, A. 2023, *ApJ*, 956, 3, doi: [10.3847/1538-4357/acf4f8](https://doi.org/10.3847/1538-4357/acf4f8)
- Soria, R., Pakull, M. W., Motch, C., et al. 2021, *MNRAS*, 501, 1644, doi: [10.1093/mnras/staa3784](https://doi.org/10.1093/mnras/staa3784)
- Sridhar, N., & Metzger, B. D. 2022, *ApJ*, 937, 5, doi: [10.3847/1538-4357/ac8a4a](https://doi.org/10.3847/1538-4357/ac8a4a)
- Sun, S., Yu, W., Yu, Y., & Mao, D. 2021, *The Astrophysical Journal*, 907, 25, doi: [10.3847/1538-4357/abd477](https://doi.org/10.3847/1538-4357/abd477)
- Sun, S., Yu, W., Yu, Y., Mao, D., & Lin, J. 2019, *The Astrophysical Journal*, 885, 55, doi: [10.3847/1538-4357/ab4420](https://doi.org/10.3847/1538-4357/ab4420)
- Wenger, M., Ochsenein, F., Egret, D., et al. 2000, *A&AS*, 143, 9, doi: [10.1051/aas:2000332](https://doi.org/10.1051/aas:2000332)
- Wolter, A., Rushton, A., Mezcua, M., et al. 2015, in *Advancing Astrophysics with the Square Kilometre Array (AASKA14)*, 91, doi: [10.22323/1.215.0091](https://doi.org/10.22323/1.215.0091)
- Yang, Y.-P., & Zhang, B. 2018, *ApJ*, 868, 31, doi: [10.3847/1538-4357/aae685](https://doi.org/10.3847/1538-4357/aae685)
- Zhang, B. 2020, *Nature*, 587, 45, doi: [10.1038/s41586-020-2828-1](https://doi.org/10.1038/s41586-020-2828-1)
- . 2023, *Reviews of Modern Physics*, 95, 035005, doi: [10.1103/RevModPhys.95.035005](https://doi.org/10.1103/RevModPhys.95.035005)
- Zhang, X., Yu, W., Law, C., et al. 2023, *ApJ*, 959, 89, doi: [10.3847/1538-4357/ad0545](https://doi.org/10.3847/1538-4357/ad0545)

APPENDIX

Table 4. The observations for *Swift*/BAT event data analysis

obsID	start time (UTC)	exposure (seconds)
00968731000	2020-04-30 12:53:02	120
00972010000	2020-05-13 13:23:32	272
00972011000	2020-05-13 13:33:27	1023
00972030000	2020-05-13 14:51:48	1142
00973140000	2020-05-19 11:16:44	1202
00088915014	2020-05-20 14:10:19	200
00973140006	2020-05-22 15:36:09	200
00974942000	2020-05-29 00:52:56	1122
00975895000	2020-06-03 19:25:16	1202
00089076001	2020-07-14 05:55:33	121
00095656005	2020-07-18 08:24:09	200
00013597029	2020-08-23 11:13:08	200
00095660154	2020-09-16 06:01:40	200
00996184000	2020-09-17 03:48:49	1202
00996184003	2020-09-19 14:58:12	200

Table 5. The properties of the detected FRB bursts during *Swift* observations.

Burst time ^a (MJD)	DM (pc cm ⁻³)	Pulse width (ms)	Energy ($\times 10^{37}$ erg)
58991.7289360891	1214.2	30.2	16.8
59067.484346541	1202.8	14.9	15.9
59067.4843471197	1202.8	33.1	17.8
59071.470504066	1200.0	5.2	9.6
59071.4705042975	1200.0	7.2	8.1
59075.4527133255	1210.6	24.9	38.0
59075.453222841	1210.6	22.0	25.5
59077.496363178	1218.6	15.3	16.8
59077.4965143868	1218.6	13.6	10.9
59077.497517645	1218.6	4.6	11.4

^a The burst time is at Coordinated Universal Time (UTC), which is referenced to 1.5 GHz.